RSC Advances

ROYAL SOCIETY OF CHEMISTRY

www.rsc.org/advances

Determination of Diltiazem in the presence of Timolol in human serum samples using a nanoFe_3O_4@GO modified glassy carbon electrode

Mohammad Hasanzadeh [a], Mohammad Hossein Pournaghi-Azar [b], Nasrin Shadjou [c, d]

Abolghasem Jouyban [a*1]

[a] Drug Applied Research Center and Faculty of Pharmacy, Tabriz University of Medical Sciences, Tabriz 51664, Iran.

[b] Electroanalytical Chemistry Laboratory, Faculty of Chemistry, University of Tabriz, Tabriz, Iran.

[c] Department of Nanochemistry, Nano Technology Center, Urmia University, Urmia, Iran.

[d] Department of Chemistry, Faculty of Science, Urmia University, Urmia, Iran.

[*] Corresponding author: Tel.: +98 411 3379323; fax: +98 411 3363231.

E-mail address: ajouyban@hotmail.com

Abstract

A new chemically modified electrode was constructed based on a magnetic graphene oxide modified glassy carbon electrode (nanoFe_3O_4@GO-GC). At the first time, the electrode was evaluated as an electrochemical sensor for simultaneous determination of diltiazem and timolol in aqueous solutions. The measurements were carried out by application of the differential pulse voltammetry method in phosphate buffer solution with pH 6.00. The results revealed that nanoFe_3O_4@GO promotes the rate of oxidation by increasing the peak current. NanoFe_3O_4 loaded in GO can increase anodic peak currents of diltiazem and timolol on electrode surface. The electrostatic interaction between diltiazem and timolol cations and the high electron density of hydroxyl groups of nanoFe_3O_4@GO would lead to increase in concentration of diltiazem and timolol around the surface of the modified electrode and the peak current increased significantly. The prepared electrode shows voltammetric responses with good selectivity for diltiazem and timolol in optimal conditions, which makes it very suitable for simultaneous determination of these drugs. The practical analytical utility of the modified electrode was illustrated by simultaneous determination of diltiazem and timolol in spiked serum samples.

Keywords: Diltiazem, Timolol, Electrochemical nanosensor, Magnetic nanoparticle, Pharmaceutical analysis

1. Introduction

Electrochemical techniques have been used for the determination of a wide range of drug compounds, often without derivatization. [1] Additionally, electrochemical techniques include the determination of the drug's electrode mechanism. [2] Redox properties of drugs can provide insight into their metabolic fate, their *in vivo* redox processes and their pharmacological activity. [3, 4] For that reasons, it is important to find more sensitive sensors for detection of drugs.

One of the best materials for construction of electrochemical sensors is graphene oxide (GO). GO, as a basic material for the preparation of individual graphene sheets in bulk-quantity, has attracted great attention in recent years. [5-7] In addition, the incredibly large specific surface area (two accessible sides), the abundant oxygen containing surface functionalities, such as epoxide, hydroxyl, and carboxylic groups, and the high aqueous solubility afford GO sheets great promise for many applications. [4-7] The intrinsic oxygen-containing functional groups were used as initial sites for deposition of metal nanoparticles, such as Fe_3O_4, on the GO sheets, which opened up a novel route to multifunctional nanometer scaled catalytic, magnetic, and electronic materials. [8-11] However, few studies about the drug monitoring by GO have been reported to date.

Determination and quantification of drugs in biological fluids and pharmaceutical samples are essential in pharmaceutical, toxicological, doping and clinical chemistry research. [12] Cardiovascular drugs encompass a large number of prescription medications that are used to control heart disease. It is a complicated group of drugs with many being used for multiple heart conditions which are good reason to have a sensitive sensor for determination of these drugs in spiked serum samples. [13] The therapeutic efficacy is

related to the interference effect of cardiovascular drugs in biological fluids and pharmaceutical samples**.** Therefore, the simpler and more rapid methods for simultaneous analysis of several cardiovascular drugs are interesting for therapeutic drug monitoring purposes. [14] Despite their widespread application and use, little works has been reported on the simultaneous determination of cardiovascular drugs by electrochemical and the related sensing devices. Therefore, simultaneous determination of these drugs is necessary for better management of pharmacotherapy of heart diseases.

Previous studies show significant cardiovascular risk associated with hypertension and control of hypertension has impressive effects on the health status. Mono therapy approach to manage the hypertension could not provide desired results and less than one third of the hypertensive patients achieved the desired blood pressure. [15] The combination of thiazides, b-blockers, acetyl choline esterase (ACE) inhibitors and calcium channel blockers are the well-studied combination therapy and showed that lowering the dose of these drugs by combining two or more will lead to higher efficacy and lower side effects. On the other hand, the newer classes such as angiotensin II receptor antagonists also used in combination with other classes but their effects have not well evaluated. [16]

Quantification of the cardiovascular drug was studied widely in combined drug therapy. Recently the quantification of a set of drugs used in combined drug therapy of cardiovascular diseases was studied with two different methods. [17, 18] The review of the published papers showed that several analytical methods were developed for simultaneous determinations of these drugs which are usually used in combination therapy protocols, where simultaneous analyses of these drugs family have been studied rarely [17, 18]. It is established that timolol (TM) increased the risk of atrio-ventricular (AV)

block and bradycardia when given with diltiazem (DT). [19] Regarding to the different mechanism of actions of these drugs, their combination in different ways, are among the interested therapy strategies for cardiovascular disease. As far as we are aware, there is no report on determination of DT in the presence of TM by electrochemical methods in biological samples. In the present work, we constructed a new magnetic electrochemical sensor for detection of DT in the presence of TM. The present study was an attempt on the development and application of the modified electrodes which were aimed at inspecting of the electrochemical processes of these important drugs. NanoFe_3O_4@GO used as modifier material and studied the electrochemical oxidation and determination of DT and TM at nanoFe_3O_4@GO modified glassy carbon electrode (NanoFe_3O_4@GO-GCE). To the best of our knowledge, this is the first report of the determination of DT in the presence of TM based on their direct electrochemical oxidation on graphene or its derivatives.

2. Experimental

2.1. Chemical and Reagents

All of chemicals were purchased from Merck (Darmstadt, Germany) and used without further purification. The drugs involved were obtained as a gift from Sobhan Darou Co., (Rasht, Iran). The standard solution of authentic drugs was prepared by dissolving an accurate mass of the bulk drug in an appropriate volume of 0.1 M phosphate buffer solution, pH 6.00 (PBS) (which was also used as supporting electrolyte), and then stored in the dark place at 4 °C. Additional dilute solutions were prepared daily by accurate dilution just before use. De-ionized (DI) water was used for preparation of aqueous solutions.

2.2. Serum sample preparation

Drug-free serum samples were obtained from healthy volunteers and stored frozen until the assay. The serum samples were diluted (1:2) with the supporting electrolyte and filtrated through a 5 μm filter to produce protein-free human serum. Various portions of stock DT and TM solution were transferred into 10 mL volumetric flasks containing 3.0 mL of the serum sample. These solutions were diluted to the mark with the supporting electrolyte for preparation of spiked samples (final dilution of 1:3 with the supporting electrolyte). The protein-free spiked serum solutions were directly analyzed by the calibration method, according to our proposed procedure.

2.3. Apparatus

Electrochemical measurements were carried out in a conventional three-electrode cell (from Metrohm) powered by an electrochemical system comprising of AUTOLAB system with PGSTAT302N (Eco Chemie, Utrecht, The Netherlands). The system was run on a PC using NOVA 1.7 software. The ac voltage amplitude used was 10 mV and the equilibrium time was 5 s. An Ag/AgCl-Sat'd KCl (from Metrohm) and a platinum wire were used as reference and counter electrodes, respectively. The working electrode was a glassy carbon (GC) electrode (from Azar Electrode Co., Urumia, Iran) and nanoFe_3O_4@GO -GC electrode, exposing a geometric surface area of 0.0314 cm^2. For differential-pulse voltammetry (DPV) measurements, a pulse width of 25 mV, a pulse time of 50 ms, and a scan rate of 5 mVs^{-1} were employed.

FT-IR spectra were recorded on a Shimadzu model FT-IR prestige 21 spectrophotometer using KBr discs. X-ray powder diffraction (XRD) measurements were

performed using a Philips diffractometer manufactured by X'pert with monochromatized Cu K_α radiation

2.4. Synthesis of the nanoFe_3O_4@GO

The GO was prepared from purified natural graphite using modified Hummer method, [20] where graphite powder (0.5 g) was added to 50 mL of 98% H_2SO_4 in an ice bath, then $KMnO_4$ (2 g) was gradually added while stirring. The rate of addition was controlled carefully, avoiding a sudden increase of temperature. The stirring was continued for 2 h at temperatures below 10 °C, followed by 1 h at 35 °C. Then the reaction mixture was diluted with 50 mL of DI water in an ice bath where the temperature was kept below 100 ◦C. The mixture was stirred for another 1 h, and further diluted to approximately 150 mL with DI water. After that, 10 mL of 30% H_2O_2 was added to the mixture which changed its color to brilliant yellow. The resultant was centrifuged and washed several times with 5% HCl aqueous solution, then by DI water until the pH of the supernatant become neutral. Finally the resulting solid was dried at 60 ◦C for 24 h where a loose brown powder, was obtained. The nanoFe_3O_4@GO composites were synthesized by co-precipitation of $FeCl_3.6H_2O$ and $FeCl_2.4H_2O$, in the presence of GO. An aqueous solution of ferric chloride and ferrous chloride was prepared in a 2:1 mole ratio. For the preparation of nanoFe_3O_4@GO, 40 mg of GO in 40 mL of water was ultrasonicated for 30 min, to which a 50 mL solution of $FeCl_3$ (110 mg), $FeCl_2$ (43 mg) and 20 mL 30% ammonia solution in DI water was added at room temperature. After completion of the addition, nanoFe_3O_4@GO was obtained as a brown powder (**Scheme 1**).

2.5. Characterization of nanoFe_3O_4@GO

The general morphologies of synthesized nanoFe_3O_4@GO were observed by SEM and shown in **Fig. 1**. A flat surface was shown in **Fig. 1A**, which demonstrating a single atomic layer thickness structure feature. The properties of nanoFe_3O_4@GO are highly related to their micro structures, their dispersity and the morphology of Fe_3O_4 nanoparticles. The presence of Fe_3O_4 nanoparticles in GO surface was confirmed by SEM **(Fig. 1A**). In contrast to the surface of GO which was quite smooth, the added Fe_3O_4 nanoparticles to GO appeared as bright dots, which were spread on the surface of the GO. The morphology of nanoFe_3O_4@GO was examined by TEM (**Fig. 1B**), where the image of prepared composite showed Fe_3O_4 nanoparticles as nearly spherical and homogeneously distributed over the GO nanosheets.

In FT-IR spectra the band in the region of 400-650 cm^{-1} is assigned to the stretching vibrations of the (Fe-O) bond in Fe_2O_3 confirming the existence of Fe_3O_4 (**Fig. 2**). Two additional bands at 1450 and 1376 cm^{-1} appeared, suggesting some interaction between the carbonyl and hydroxyl groups of GO and Fe on the surface of the magnetic particles, and showing the bonding of the iron oxide nanoparticles to GO.

The structural properties of the synthesized nanoFe_3O_4@GO were analyzed by XRD (**Fig. 3**). The diffraction peak of GO appeared at 23.94° which originated from the diffraction on its (0 0 2) layer planes. Also, synthetic nanoFe_3O_4@GO showed some low intensity diffraction peaks that were indexed to cubic Fe_3O_4. The XRD peaks of magnetic graphene-oxide were indexed to (2 2 0), (3 1 1), (4 0 0), (4 2 2) and (5 1 1) planes of a cubic unit cell of magnetite, appearing at 35.01◦, 43.27◦, 53.22◦, 58.46◦, and 63.50◦, respectively.

2.6. Preparation of the nanoFe_3O_4@GO-GCE

Prior to use, the nanoFe_3O_4@GO were sonicated in a 3:1 sulfuric/nitric acid solution for 6 h in an ultrasonic bath at room temperature and then washed with distilled water. The obtained sample was taken, and dried overnight at 50 °C. Prior to the modification, the GC electrode was polished with 0.05 µm alumina suspension on a polishing micro-cloth, followed by sonication for 5 min in an ultrasonic bath in a 1:1 ethanol/distilled water mixture. The electrode was then transferred to the 1.0 M sulfuric acid solution. Potential in the range of -1 to 1.5 V in a regime of cyclic voltammetry was applied for 20 cycles. Afterward, the electrode was rinsed thoroughly with distilled water and dried in air. (It should be noted that this pretreatment was also employed for the bare GC electrode in the experiments that the unmodified electrode was tested). nanoFe_3O_4@GO (50 mg) was dispersed into acetone/double distilled water with the aid of ultrasonic stirring for 6 h. A 10 µL aliquot of this dispersion (with concentration of 1.0 mg mL^{-1}) was dropped on the GC electrode surface, and the surface was allowed to dry in room temperature (24 h). When not in use, the electrodes were stored at 4 °C.

3. Results and discussion

3.1. Electrochemical behaviors of DT and TM

Fig. 4 (A and B) shows typical cyclic voltammograms (CV) of PBS containing 0.1 mM DT and TM using GO-GC (A) and nanoFe_3O_4@GO-GC electrodes (B). **Fig. 4A** does not show oxidation signal on GC electrode. This indicated the electroinactivity of DT and TM on the GO-GC surface. Typical CV of nanoFe_3O_4@GO-GC electrodes in 0.1 M PBS containing 1 mM DT and TM and in the potential range of -1 to 1 V is shown as **Fig. 4B** where potential sweep rate of 100 mVs^{-1} has been employed. DT and TM exhibit one oxidation peak, located at 0.98 and 0.62 using the nanoFe_3O_4@GO-GC electrode at PBS

with pH=6.00, respectively. In the reverse sweep, however, no peaks appeared, indicating an irreversible heterogeneous electron transfer process for the oxidation of DT and TM on the nanoFe_3O_4@GO-GC electrode surface. Furthermore, the peak currents enhanced significantly. These results indicated that nanoFe_3O_4@GO film could accelerate the rate of electron transfer of DT and TM and have good electro-activity for oxidation of these drugs. The possible reason is the electrostatic interaction between modifier and drugs. Hence, the electrostatic interaction between DT and TM cations and the high electron density of hydroxyl groups of nanoFe_3O_4@GO would lead to increase in concentration of analytes around the surface of the modified electrode and the peak current increased significantly.

The peak potential was closely dependent on the pH of the solution. It was found that the values of peak potential shifted to negative values with the increase of pH (as shown in **Fig. 4C**). The peak potential (Ep) moved in negative direction with pH rising and they showed such relationship as Ep= -52.219 pH + 57.784 (R^2 = 0.9892) and Ep= -51.330 pH + 55.714 (R^2 = 0.9782) for DT and TM, respectively. The slope of -52.2 mV pH^{-1} and -51.3 demonstrated that the numbers of electron and proton transferred in the electrochemical reaction of DT and TM were equal and is one.

The influence of the scan rate on the electrochemical response of DT at the modified electrode was investigated by CV. The oxidation peak currents exhibited a linear relation to the square root of the scan rate in the range between 10-700 mVs^{-1} with the linear regression equation of $I_{pa}(\mu A)=0.225(mVs^{-1})+2.390$ (R^2=0.9935). The results in **Fig. 5A** indicated that the electron transfer reactions were diffusion-controlled process. The anodic peak potential shifted positively with the increase in scan rate, indicating the

irreversible nature of the electrode reaction. The results indicated that the modified electrode could accelerate the electron transfer reaction and exhibit good electroactivity effect. The possible reaction mechanism was that DT existed as a cation with hydroxyl group of nanoFe_3O_4@GO in pH 6.00 PBS (**Scheme 2**).

Similar result was obtained for electrooxidation of TM. The CVs of 1 μM of TM at modified electrode in 0.1 M PBS (pH 6.00) at various scan rates were recorded to investigate the influence of the scan rate on the electrochemical response of TM. The results in **Fig. 6B** showed that the anodic peak currents were proportional to the square root of scan rate in the range of 10-300 mVs^{-1} with the linear regression equation of $I_{pa}(\mu A)= 0.207(mVs^{-1}) + 1.225$ (R^2=0.991) indicating that the oxidation reactions were controlled by a diffusion process. In addition, the oxidation peak potentials shifted with the increase of scan rate, which suggested that the electrode reaction of TM is irreversible. On the hand, a dependence of Ln i_p on Ln *v is* linear **(Figs. 6 A and B**) and described by the following equations:

$$\text{Ln } I_p = 0.489 \text{ Ln } v \text{ (V s}^{-1}) - 5.102 \text{ mA} \quad (R^2 = 0.991) \quad \text{TM} \quad (1)$$

$$\text{Ln } I_p = 0.543 \text{ Ln } v \text{ (V s}^{-1}) - 6.466 \text{ mA} \quad (R^2 = 0.986) \quad \text{DT} \quad (2)$$

Its slope is 0.489 (for TM) and 0.543 (for DT) and indicates diffusion control of the electron transfer process. A slope close to 0.5 is expected for diffusion-controlled process. [21, 22]

3.2. Effect of pH on the voltammetric responses of DT and TM

Since the oxidation of the selected analytes is pH dependent, in order to optimize operational condition and obtain the best peak separation and higher response, the effect of pH on electrochemical response of the nanoFe_3O_4@GO-GC electrode towards the

simultaneous determination of DT and TM solutions were investigated. The effects of pH on the oxidation responses of DT and TM at the modified electrode were studied over the pH range from 3 to 10. According to the experimental results **Fig. 6C**, the modified electrode showed good electroactivity for redox reactions of DT and TM in wide pH range. The anodic peak currents increased with increasing the pH up to 6.00, and then the peak currents decreased. The maximum peak current value can be observed at pH 6.00 for DT and TM. So it was selected as the optimum pH for the simultaneous determination of DT and TM in this study.

3.3. Simultaneous detection of binary mixture of DT and TM

Fig. 5 illustrated the CVs of the mixture containing DT and TM at modified electrode. As shown in **Fig. 7** when the modified electrode was used, the mixture was displayed a difference on peak potentials about 170 mV. Therefore, the sharp and well-defined oxidation peaks with significantly enhanced peak currents were selected for simultaneous detection of DT and TM.

The next attempt was taken to detect DT and TM simultaneously at the modified electrode by DPV because of its higher current sensitivity and better resolution than CV. **Fig. 8** illustrated the DPV responses of the modified electrode while the concentrations of DT and TM increased synchronously. It can be seen that the anodic peak currents for the two analytes increased linearly with increase of their concentrations. The analytical responses of the modified electrode toward the simultaneous determination of DT and TM were listed in **Table 1**. The proposed method had low limit of detection (LOD), wide linear range and good stability compared with other methods. As results indicate, the modified electrode can be used for sub-micromolar detection of the proposed analytes

without any pretreatment or pre-concentration steps. The comparison of this method with other electrochemical methods for the simultaneous determination of DT and TM was listed in **Table 2.** [23-27] The analytical parameters of the modified electrode such as LOD and linear concentration range are better than or even comparable with the reported data in the literature for voltammetric or amperometric detection of these selected analytes with different modified electrodes.

3.4. Analytical application

The practical analytical utility of the modified electrode was illustrated by simultaneous determination of DT and TM in serum samples.

The generally poor selectivity of voltammetric techniques can pose problems in the analysis of biological samples, which contain oxidizable substances. However, no current due to oxidation of the drugs in the serum samples appeared. 1.00 mL of DT (specified content of DT is 10 mg mL^{-1}) and 5.00 mL TM (specified content of TM is 1 mg mL^{-1}) injection were diluted to 50mL with buffer solution, respectively. Different capacity diluted solutions were pipetted into each of series of 10 mL volumetric flasks and diluted to the mark with 0.1 M PBS (pH 6.00). Then this test solution was placed in the electrochemical cell. The proposed DPV method was used to simultaneous detection of DT and TM. The average determination results of DT and TM in the spiked serum samples were 9.44 and 0.93 mg mL^{-1}, which were almost corresponding to the values that were given by injection specifications. This process was repeated for 10 times, and RSDs obtained for DT and TM were 1.80% and 2.13%, respectively.

To a series of 5, 10 and 20 mL measuring flasks, different capacity diluted DT and TM injection solutions was added and diluted to the mark with 0.1 M PBS (pH 6.00). The

DPVs were recorded and the anodic peak currents were measured for DT and TM. The obtained results were shown in Table 3. It can be seen that the proposed method has a good precision and can be applied to the simultaneous determination of DT and TM.

3.5. Reproducibility and stability

To verify the reproducibility, durability and long-term stability of the prepared sensor, consecutive amperograms in three concentrations of DT and TM were recorded. Fig. 9 A and **B** shows the repeatability and reproducibility of the amperometric responses to successive injections of DT and TM. The relative standard deviations (RSD) of the amperometry currents of 1, 1.5 and 2 μM of DT were 3.4%, 1.0 and 0.8% (n=6), respectively, revealing acceptable reproducibility of the method. Also, The RSD for three replicate determination of TM was 3.3, 0.5 and 5.0 % (n=6) at concentrations of 1, 1.5 and 2 μM, respectively. Obtained RSD using amperograms of DT and TM indicated that the fabrication method was reproducible and repeatable. In addition, the stability of the modified electrode was investigated by amperometric method (Fig. 9C). When the modified electrode was stored in the atmosphere, the current response decreased ~15% after 30 s. This indicates negligible fouling of the nanoFe_3O_4@GO surface by DT and TM and oxidation products. Therefore, nanoFe_3O_4@GO showed high stability and strong mediation properties for amperometric measurements of DT and TM.

3.6. Interference Studies

In order to evaluate the selectivity of the developed DPV procedure, the influence of various interferences was examined. Considerable interference can be caused by co-existing surface-active compounds capable of competing with the analytes of interest for the adsorption site on the electrode surface, resulting in decreased or in-creased peak

height. The competitive co-adsorption interference was evaluated in the presence of various substance usually occur in the biological fluids. For these investigations, the interfering species were added at different concentrations (1, 2, 5 and 50-fold) higher than the concentration of DT and TM (1 μM). The addition of 50-fold of sucrose in the test drugs solution, caused the DPV peak current to decrease by about 8%. Apparently, these inhibition effects were caused by the working electrode surface blockage due to adsorption of interferences. In contrast, the addition of 50-fold of lactose in the drug solution, caused the DPV response of the drug to increase by about 16%. In addition, the addition of 2-fold of some amino acids (Glycine, Cysteine, Tyrosine) in the test drug solution (1 μM), caused the DPV peak current to decrease by about 10%, 10%, 24%, respectively. On the other hand, the addition of ascorbic acid (5-fold) in the DT and TM solution caused the DPV response of the drug to decrease by about 14% and 10%, respectively.

4. Conclusions

In the present study, a sensitive, inexpensive, and rapid method for simultaneous determination of DT and TM was proposed based on electrooxidation of the proposed analytes on the nanoFe_3O_4@GO-GC electrodes. The proposed electrode was used for determination of DT and TM in PBS, without the necessity for sample pretreatment or any time-consuming extraction or evaporation steps prior to the analysis, with satisfactory recovery. The good stability, wide linear concentration range, low detection limit, and a distinct advantage of polishing in the event of surface fouling, suggest that this electrode is an attractive candidate as a transducer for practical applications. Also due to the large surface area of GO and remarkable electroactivity properties of Fe_3O_4,

nanoFe_3O_4@GO-GC electrode can be used for simultaneous determination some of other drugs which are necessary for interference study.

Acknowledgments

This is a report of a database from the thesis entitled "Development of sensitive, routine and reliable methods for determination of cardiovascular drugs in biological samples" registered in Drug Applied Research Center. We gratefully acknowledge the financial support of this work by the Drug Applied Research Center, Tabriz University of Medical Sciences.

5. References

1. PT. Kissenger, WR. Heineman (Eds.), Laboratory Techniques in Electroanalytical Chemistry, Marcel Dekker, New York, 1996.
2. J. Wang (Ed.) Electroanalytical techniques in clinical chemistry and laboratory medicine, VCH Publishers, New York, 1996.
3. R. Kellner, JM. Mermet, M. Otto, M. Valcarcel, HM. Widmer, Analytical Chemistry: A modern approach to analytical science, 2nd Ed. Weinheim: Wiley-VCH, 2004.
4. B. Uslu, SA. Ozkan, *Anal. Let.* 2011, ***44***, 2644-2702.
5. D. Li, MB. Muller, S. Gilje, RB. Kaner, GG. Wallance, *Nature Nanotechnol*. 2008, ***3***, 101-105.
6. S. Park, RS. Ruoff, *Nature Nanotechnol*. 2009, ***4***, 217- 224.
7. VC. Tung, MJ. Allen, Y. Yang, RB. Kaner, *Nature Nanotechnol*. 2009, ***4***, 25-29.
8. Z. Liu, JT. Robinson, X. Sun, H. Dai, *J. Am. Chem. Soc*. 2008, ***130***, 10876-10887.
9. JR. Lomeda, CD. Doyle, DV. Kosynkin, W. Hwang, JM. Tour, *J. Am. Chem. Soc.* 2008, ***130***, 16201-16206.
10. R. Muszynski, B. Seger, PV. Kamat, J. Phys. Chem. C 2008, ***112***, 5263-5266.
11. Y. Xu, Z. Liu, X. Zhang, Y. Wang, J. Tian, Y. Huang, Y. Ma, X. Zhang, Y. Chen, *Adv. Mater.* 2009, ***21***, 1275-1279.
12. BG. Katzung, Basic and clinical pharmacology, 6th ed., Appleton and Lange, California, 1995, p. 178.
13. A. Capucci, D. Aschieri, *Eur. Heart J. Suppl.* 2003, 5, H8-H11.
14. S. Li, G. Liu, J. Jia, Y. Liu, C. Pan, C. Yu, Y. Cai, J. Ren, *J. Chromatogr. B* 2007, ***847***, 174-181.

15. O. Gonzalez, G. Iriarte, N. Ferreir, MI. Maguregui, RM. Alonso, RM. Jimnez, *J. Pharm. Biomed. Anal.* 2009, ***50***, 630-639.

16. G. Iriarte, O. Gonzalez, N. Ferreir, MI. Maguregui, RM. Alonso, RM. Jimnez, *J. Chromatogr. B Anal. Technol. Biomed. Life Sci.* 2009, ***877***, 3045-3053.

17. SC. Sweetman (Ed.), Martindale, The Complete Drug Reference, 35th ed., Pharmaceutical Press, London, 2007.

18. JM. Neutel, *Nephrol. Dial. Transplant,* 2006, ***21***, 1469-1474

19. K. Apurv, BW. William, *Am J Med,* 2009, ***122***, 215-221.

20. WS. Hummers, RE. Offeman, J. Am. Chem. Soc. 1958, ***80***, 1339.

21. AJ. Bard, LR. Faulkner, Electrochemical Methods. New York, Wiley, 2001, pp. 236, 503, 709

22. CMA. Breet, AMO. Breet, Electrochemistry: Principles, Methods and Applications, Oxford University Press, New York, 1993, p. 427.

23. MR. Ganjali, T. Razavi, R. Dinarvand, S. Riah, P. Norouzi, *Int. J. Electrochem. Sci.* 2008, ***3***, 1543-1558

24. P. Norouzi, MR. Ganjali, B. Larijani, A. Mirabi-Semnakolaii, FS. Mirnaghi, A. Mohammadi, *Pharmazie* 2008, ***63***, 633-637.

25. AF. Al-Ghamdi, *Am. J. Anal. Chem.* 2011, ***2***, 174-181

26. A. Arranz, I. Dolara, A. de BetonÄo SfernaÂndez, JM. Moreda, A. Cid, JF. Arranz, *Anal. Chim. Acta,* 1999, ***389***, 225-232

27. MH. Türkdemir, G. Erdögdu, T. Aydemir, AA. Karagözler, AE. Karagözler, *J. Anal. Chem.* 2001, ***56***, 1047-1050

Table 1: Analytical parameters obtained from determination of DT and TM on nanoFe_3O_4@GO-GC electrode

Method	Drug	Linear concentration range (μM)	LOD (μM)	Linear regression (R^2)
DPV	DT	0.1-100	0.06	0.9910
	TM	0.1-340	0.02	0.9907

Table 2: Analytical parameters for detection of DT and TM for several methods

Drug	Method	Linear concentration range (μM)	LOD (μM)	Ref.
DT	potensiometry	10 to 10000	3.2	23
DT	CV	1-41450	0.29	24
TM	SW-AdSV	0.1 to 1.5	0.0126	25
	AdS-SWV	0.001 to 0.12	0.006	26
		0.012 to 0.1		
	SWP	0.04 to 3.0	0.025	
TM	DPV	1 to 5	2.5	27
DT	DPV	0.1 to 100	0.06	This Work
TM		0.2 to 340	0.02	

Table 3: Determination of DT and TM in spiked serum samples (n=6).

DT added (μM)	TM added (μM)	DT			TM		
		found (μM)	recovery	RSD (%)	found(μM)	recovery	RSD (%)
5	5	5.08	101.6	2.4	4.78	95.6	3.0
10	10	10.6	106	2.0	9.50	95	3.21
20	20	19.44	97.2	3.1	19.49	97.4	3.0

Figure legends:

Fig. 1: The SEM (**A**) and TEM (**B**) images of nanoFe_3O_4@GO.

Fig. 2: FT-IR spectra of nanoFe_3O_4@GO.

Fig. 3: XRD pattern of nanoFe_3O_4@GO.

Fig. 4: Cyclic voltammograms of 0.1 M PBS containing 0.1 mM DT and TM at (**A**) GO-GC and nanoFe_3O_4@GO-GC (**B**) electrodes. Potential sweep rate was 100 mVs^{-1}. **C**) Influence of pH on the oxidation Potential of 0.01 mM TM (A) and DT (B)

Fig. 5: A) Cyclic voltammograms of nanoFe_3O_4@GO-GC electrode in the presence of DT in different scan rates (from inner to outer): 10, 20, 30, 40, 50, 70, 100, 150, 200, 300, 350, 400, 450, 500, 550, 600, 650 and 700 mVs^{-1}). **Inset:** Peak current *vs.* scan rate. **B)** Cyclic voltammograms of nanoFe_3O_4@GO-GC in the presence of TM in different scan rates (from inner to outer): 10, 20, 50, 70, 100, 150 and 300mVs^{-1}). **Inset:** Peak current *vs.* scan rate.

Fig. 6: (A and B) Dependence of anodic peak current on the neperian logarithm of scan rate of TM and DT, respectively. **(C)** Effects of pH on peak current of DT and TM at the modified electrode. DT and TM concentration is 1 µM; scan rate: 100 mVs^{-1}.

Fig. 7: Cyclic voltammograms of nanoFe_3O_4@GO-GC electrode in 0.1 M PBS containing DT and TM with different concentrations: 0.1, 0.2, 0.3, 0.4, 0.5, 0.6, 1, 2, 5, 7, 10, 15, 20, 25, 30, 35, 40, 45 and 50 mM. Scan rate: 100 mVs^{-1}, pH=6.00.

Fig. 8: Differential pulse voltammograms of nanoFe_3O_4@GO-GC electrode in 0.1 M PBS containing DT and TM with different concentrations: 0, 0.1, 0.2, 0.3, 0.4, 0.5, 0.6, 0.7, 0.8, 0.9, 1 and 1.5 µM. scan rate: 100 mVs^{-1}, pH=6.00. **Inset:** Plot of peak current *vs.* DT and TM concentrations.

Fig. 9. Typical amperometric signals obtained during successive increments of DT (**A**) and TM (**B**) to 0.1 M PBS using the applied potential of 1.08 and 0.68 V, respectively (n=6). (**C**) The recorded chronoamperogram for 1 μM of DT (selected drug) during 30 s.

Scheme 1: Synthesis procedure of nanoFe_3O_4@GO.

Scheme 2: Oxidation mechanism of DT (**A**) and TM (**B**).

A

B

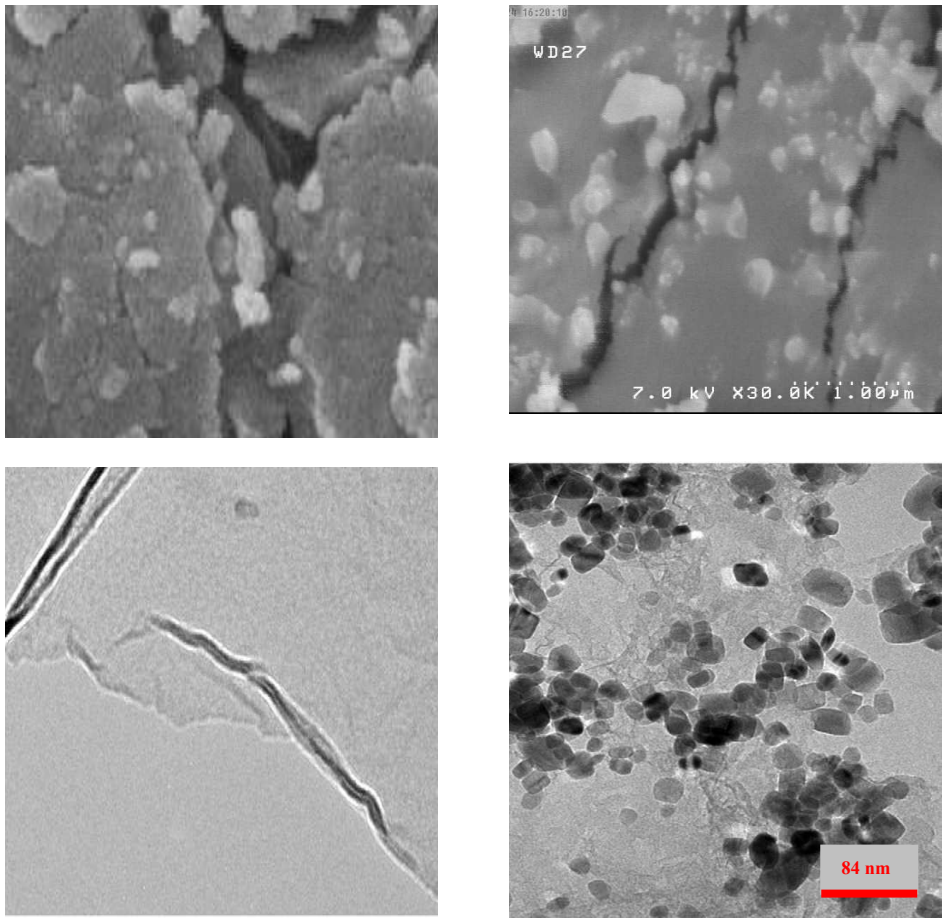

Fig. 1.

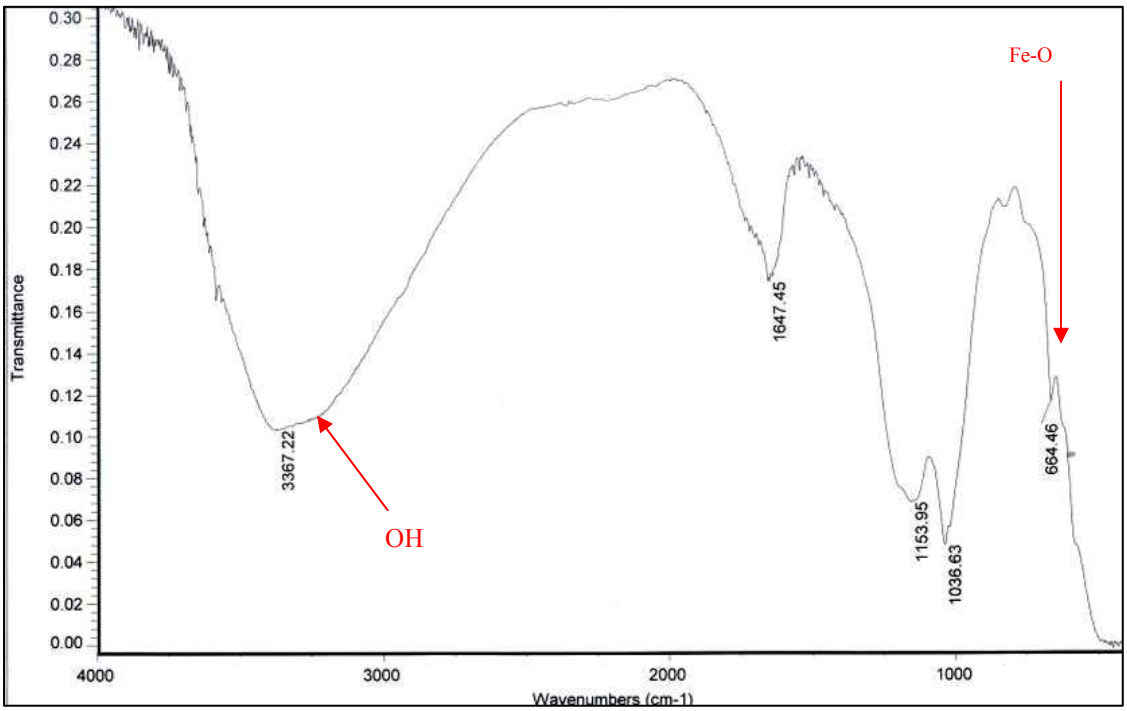

Fig. 2.

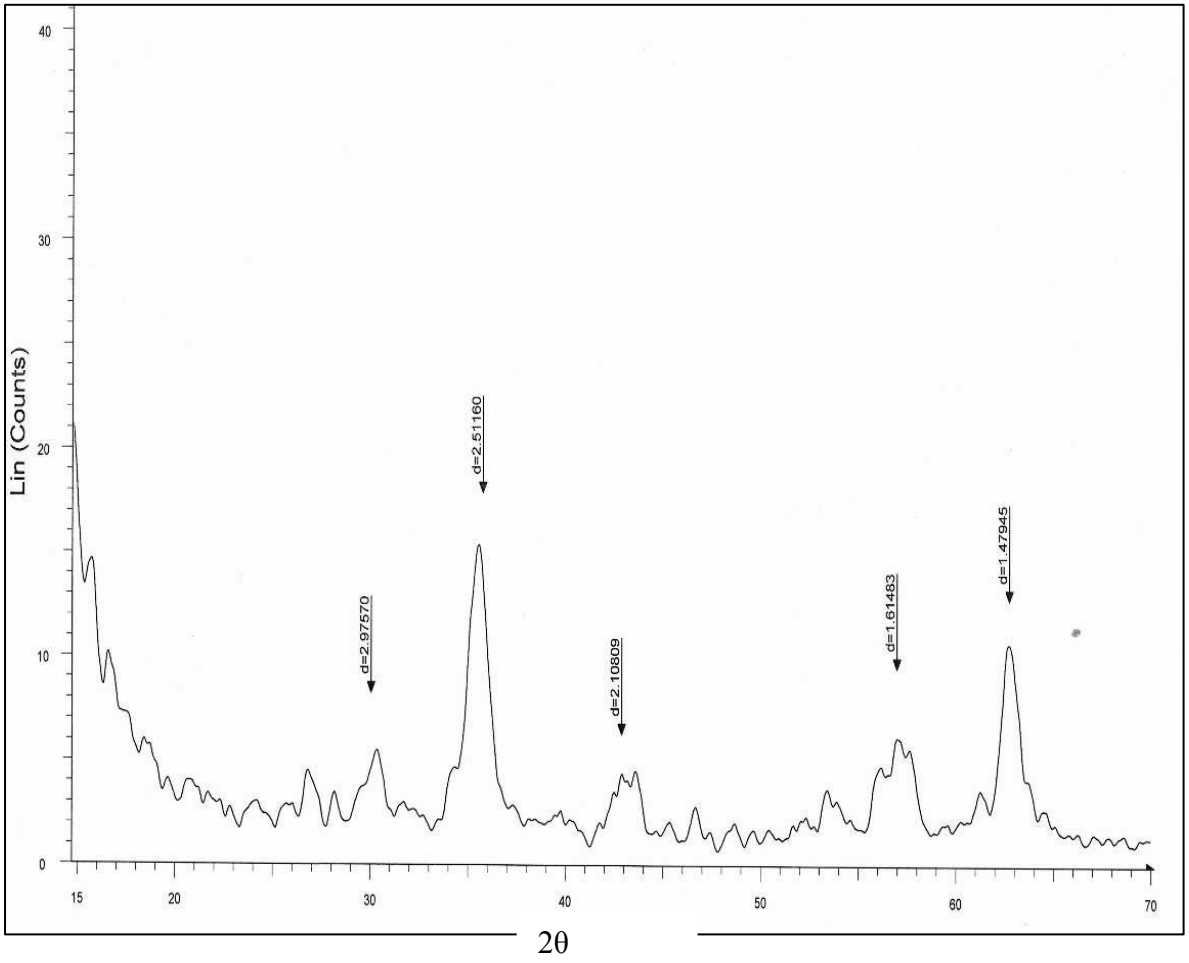

Fig. 3.

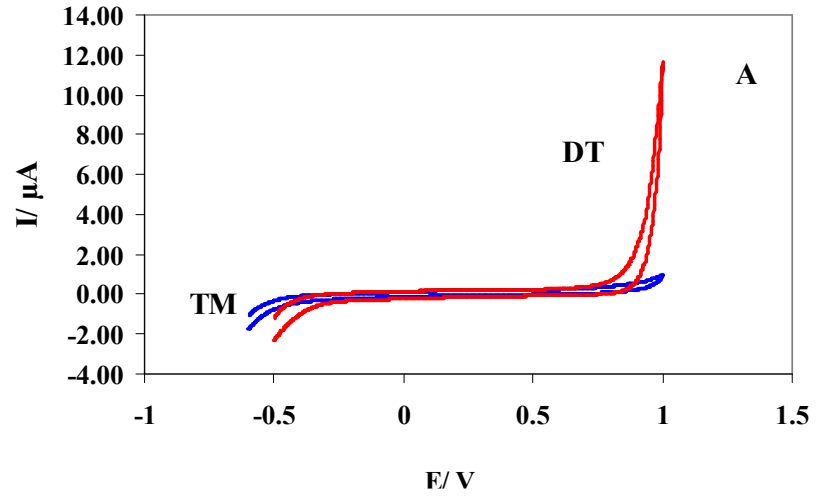

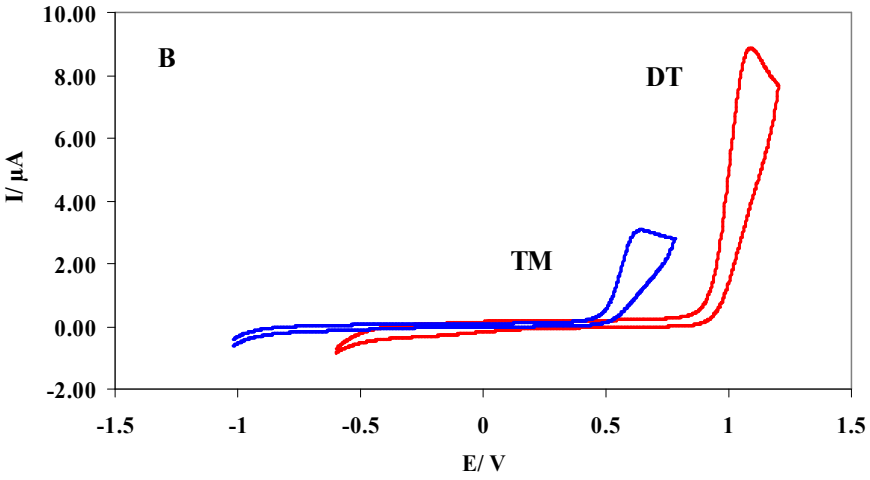

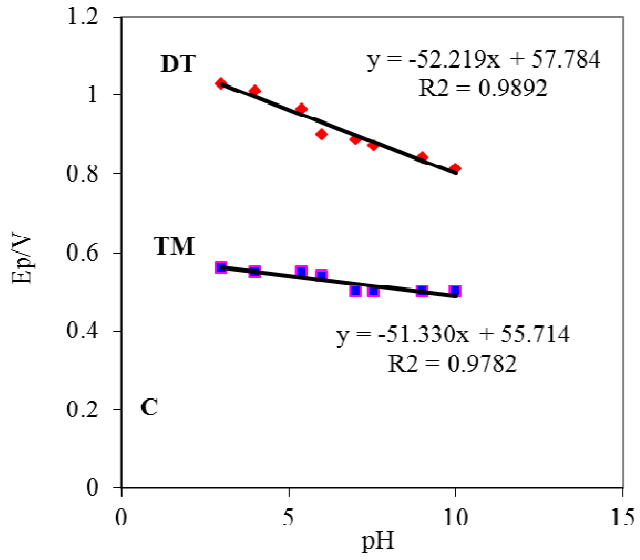

Fig. 4.

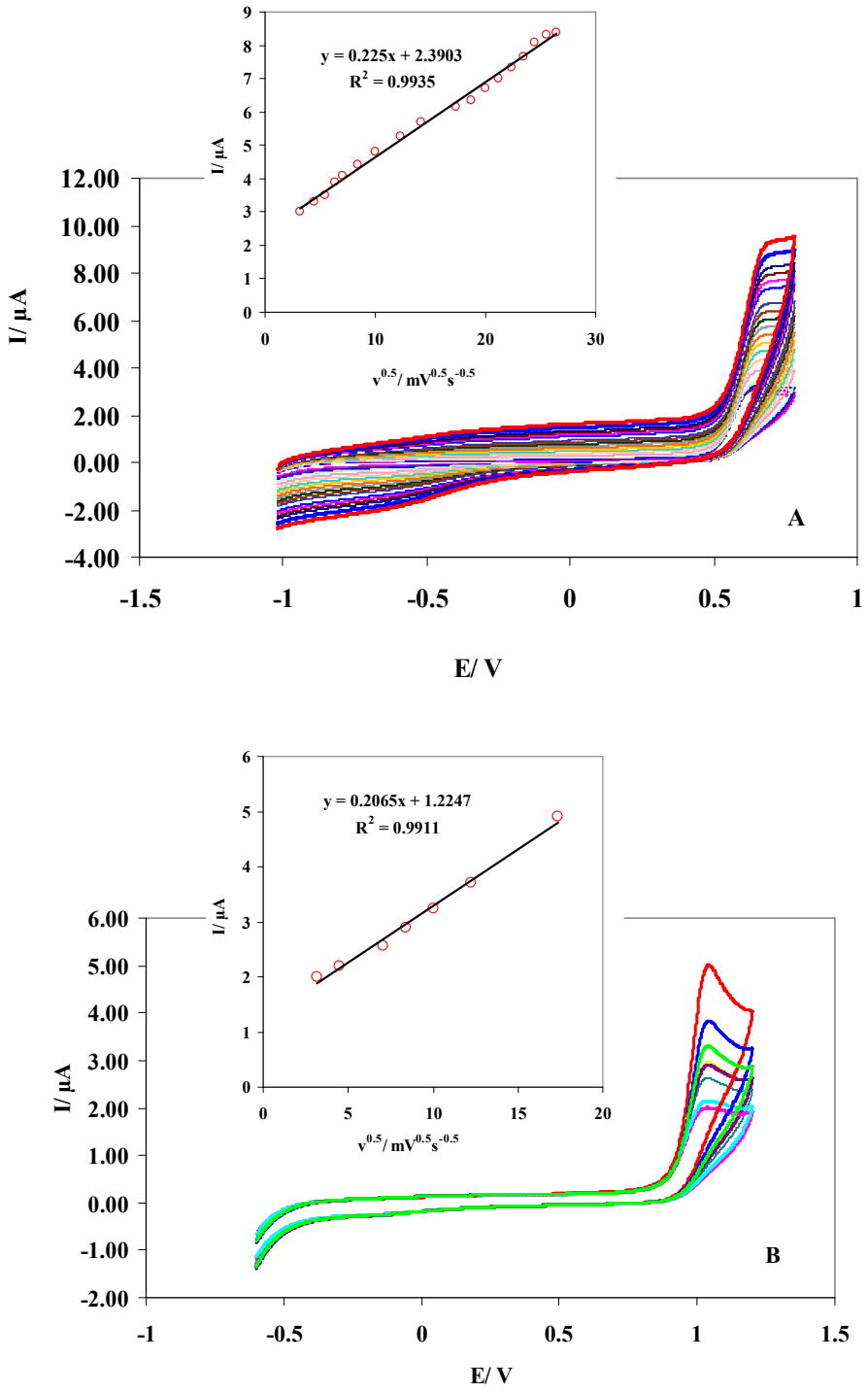

Fig. 5.

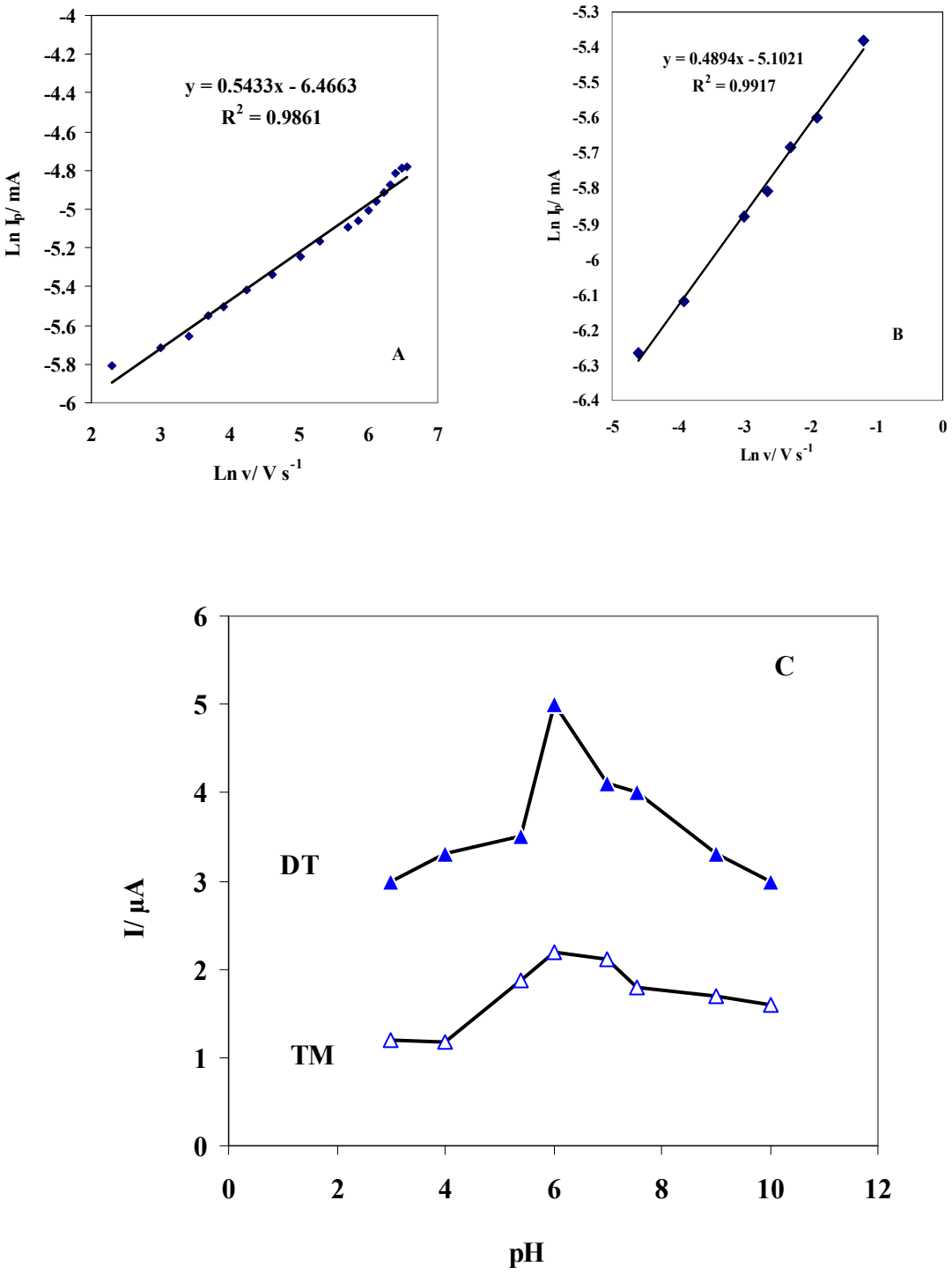

Fig. 6.

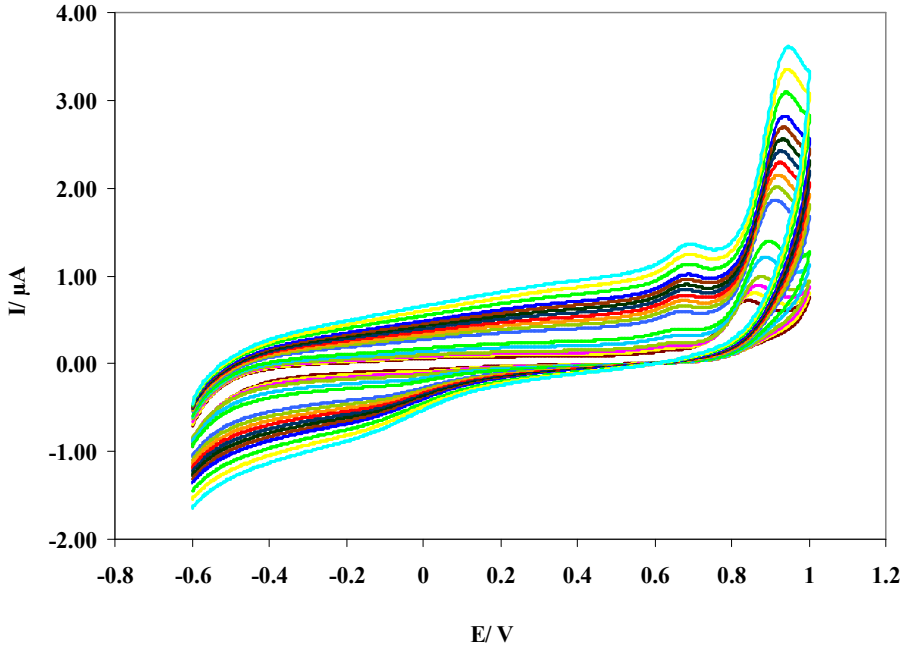

Fig. 7.

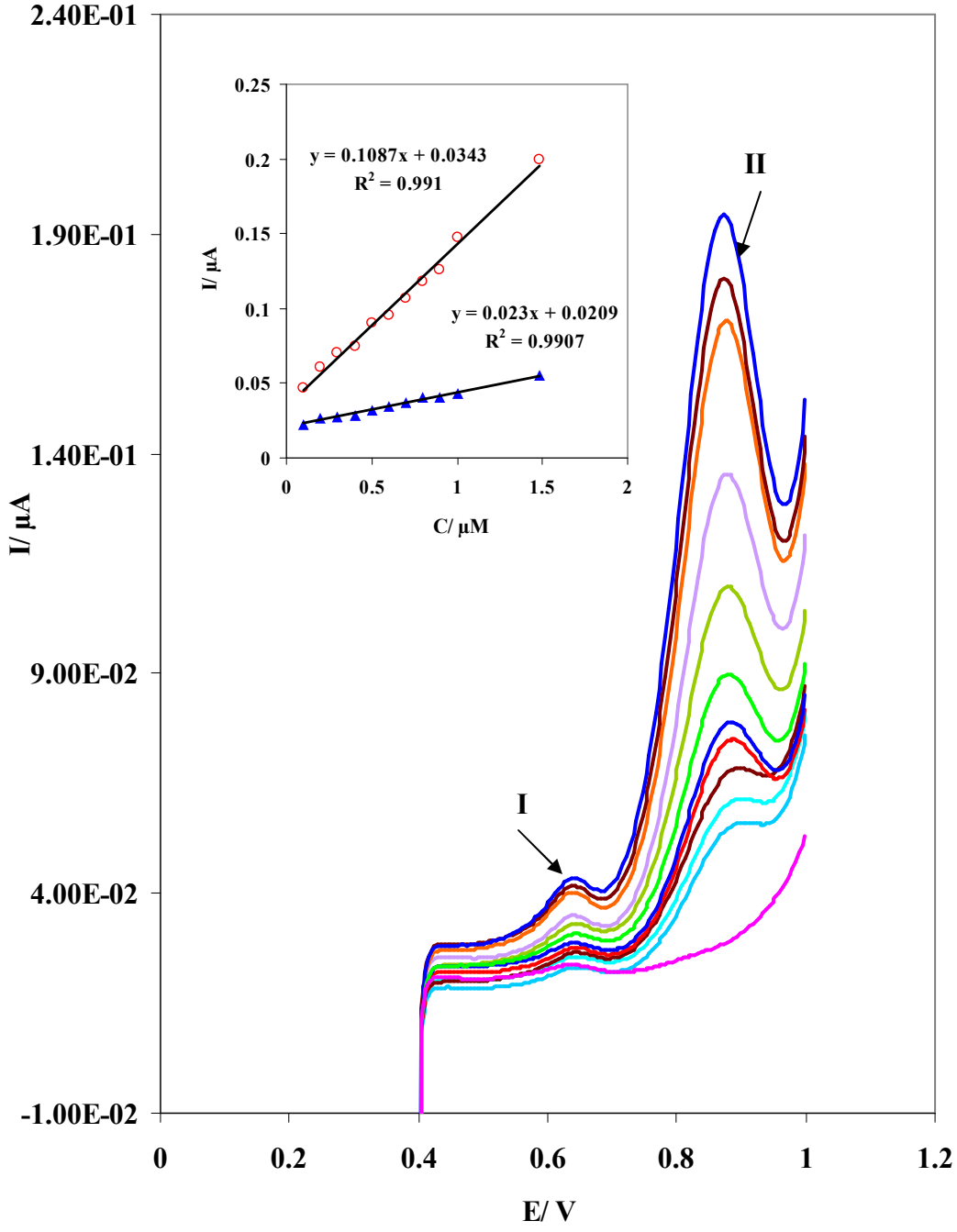

Fig. 8.

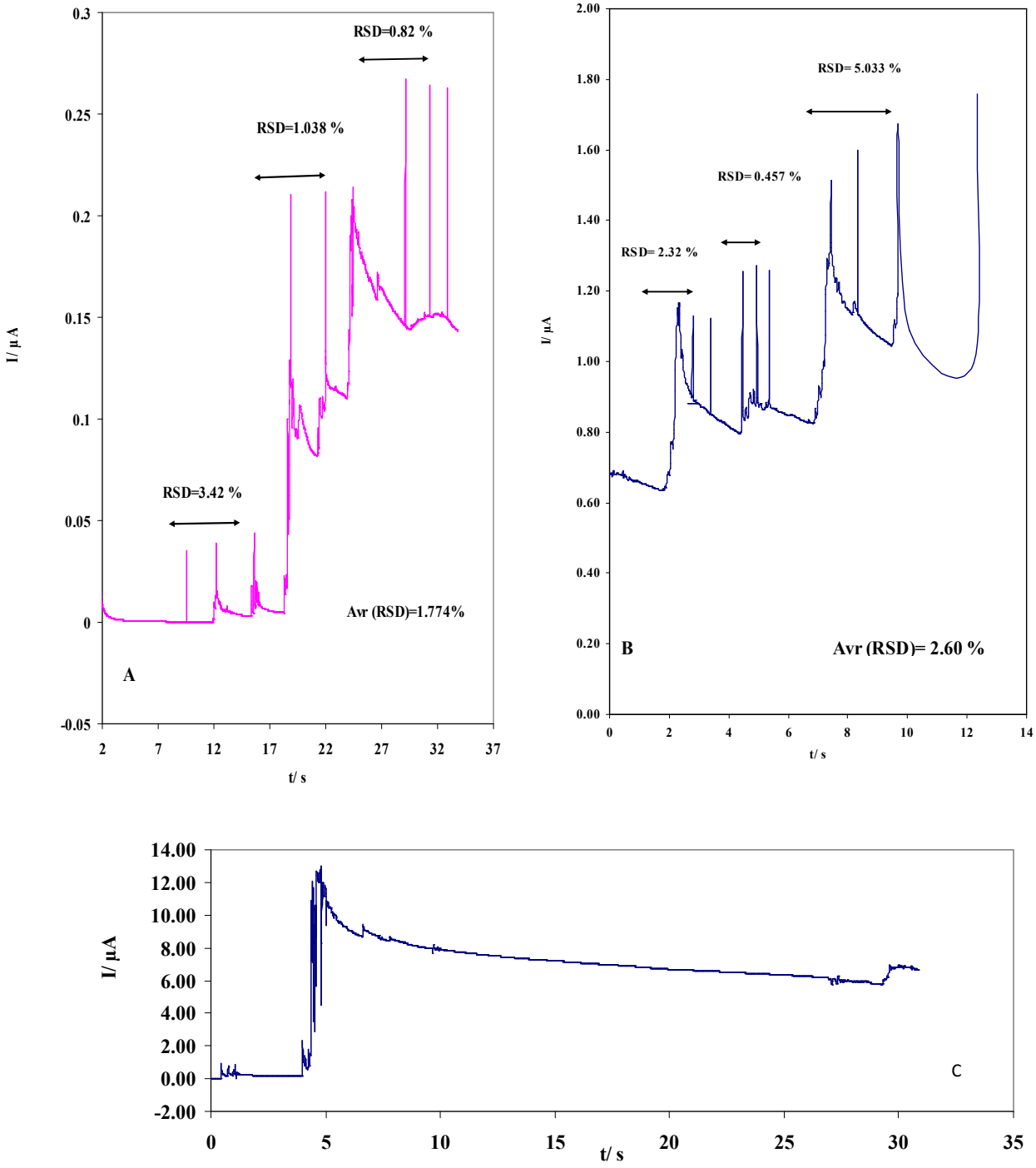

Fig. 9.

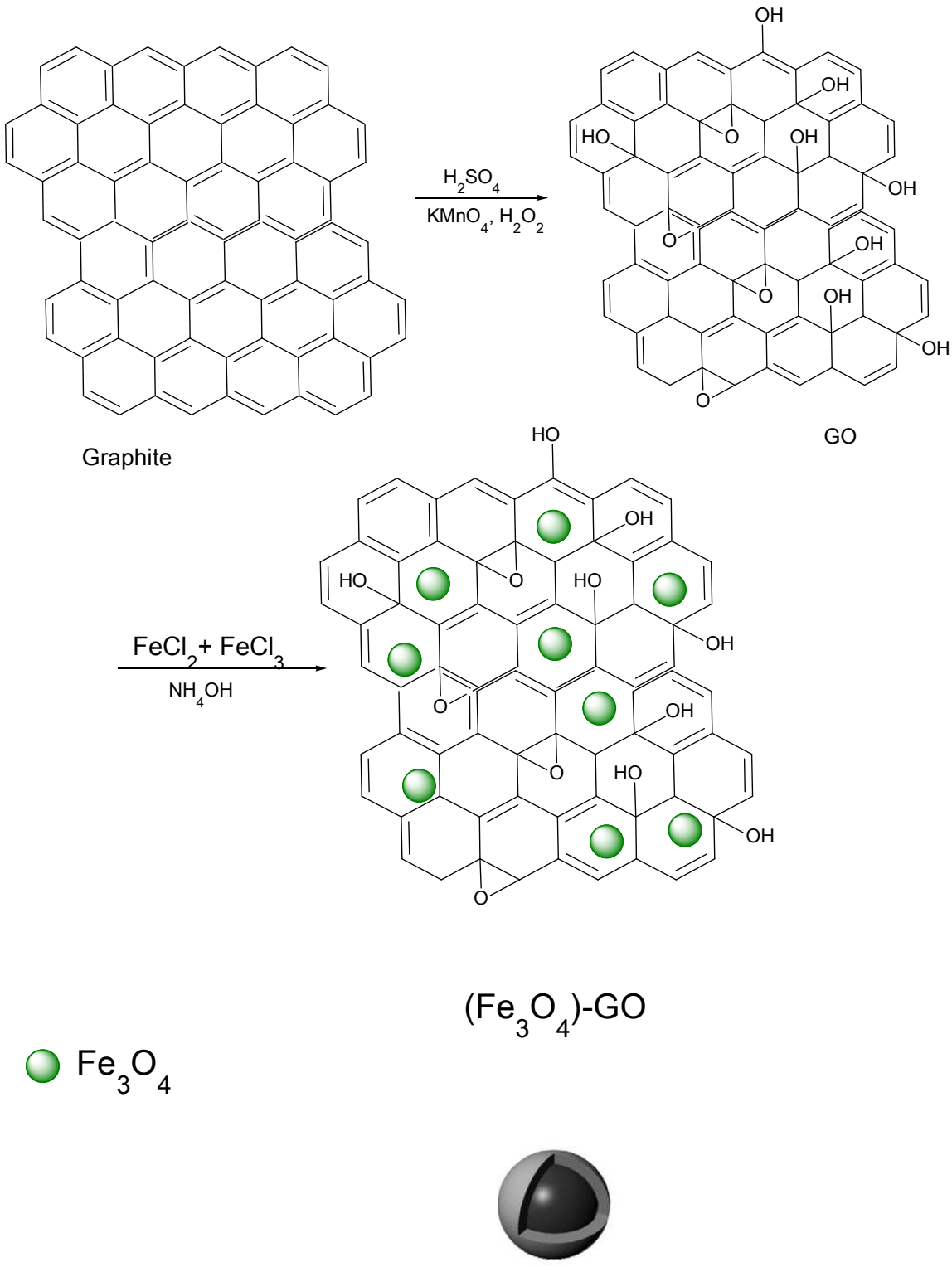

Scheme 1

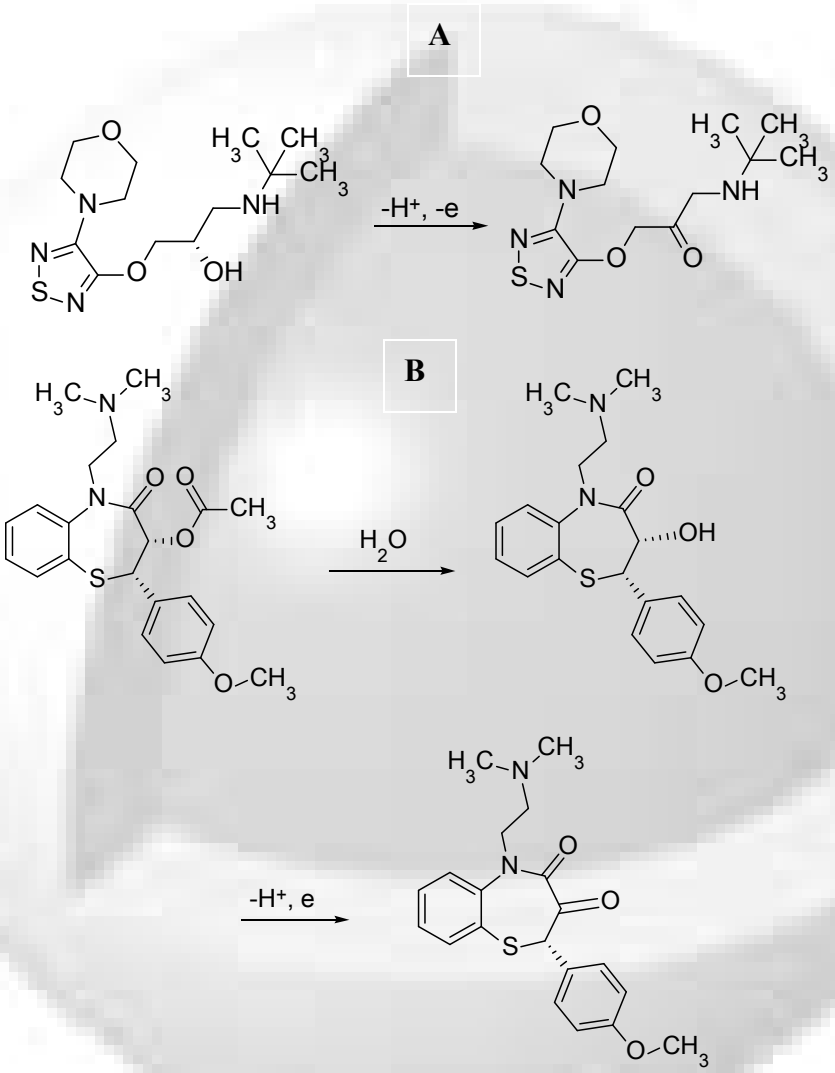

Scheme 2